C. R. Physique 14 (2013) 381–392

Contents lists available at SciVerse ScienceDirect

Comptes Rendus Physique

www.sciencedirect.com

Prix Ampère 2011 de l'Académie des sciences

Diffraction gratings: An amazing phenomenon

Réseaux de diffraction: Un curieux phénomène

Daniel Maystre

Institut Fresnel, avenue Escadrille-Normandie-Niemen, campus universitaire de Saint-Jérôme, 13397 Marseille cedex 20, France

ARTICLE INFO

Article history:
Available online 13 March 2013

Keywords:
Electromagnetic optics
Scattering
Diffraction gratings
Phenomenology
Light absorption
Perfect blazing

Mots-clés :
Optique électromagnétique
Diffraction
Réseaux de diffraction
Phénoménologie
Absorption de la lumière
Blaze parfait

ABSTRACT

The paper describes and explains the most surprising Wood's anomaly: the total absorption of a plane wave by a shallow metallic grating.
After a numerical and experimental evidence of the total absorption, we develop a quantitative phenomenological theory. Assuming that the anomalies are caused by the excitation of surface plasmon polaritons on the grating surface, we use theorems on analytic functions of the complex variable for representing the amplitudes of the scattered waves accurately through a phenomenological formula.
The original rigorous grating theory used for numerical computations is outlined and some practical applications of strong absorptions are presented.

RÉSUMÉ

Le papier décrit et explique le phénomène d'anomalie de Wood le plus surprenant : l'absorption totale d'une onde plane par un réseau métallique peu profond.
Après avoir fourni la démonstration numérique et expérimentale de l'absorption totale, nous développons une théorie phénoménologique quantitative. Prenant comme cause de l'anomalie l'excitation de plasmons polaritons de surface, nous utilisons certains théorèmes sur les fonctions analytiques de la variable complexe pour donner une expression précise des amplitudes des ondes diffractées, grâce à une formule phénoménologique.
La théorie des réseaux rigoureuse et originale utilisée pour les calculs numériques est résumée et quelques applications pratiques des fortes absorptions sont décrites.

1. Introduction

Gratings, basic instruments of spectroscopy, have played a vital role in the knowledge of the infinitely large (universe) and of the infinitely small (atomic and molecular structures) objects. However, the last decades have seen a considerable spread of the use of this instrument in science and technology. Among the new applications, a large part lies on the extraordinary resonance properties, the so-called Wood's anomalies, which are provoked by the resonant excitation of surface waves such as surface plasmon polaritons (SPP) [1]. These anomalies consist generally in strong variations of grating efficiencies or of grating absorption, generated by small variations of incidence or wavelength. The study of grating anomalies belongs to the field of plasmonics, which includes more recent (and closely linked) domains of research, for example the

E-mail address: daniel.maystre@fresnel.fr.

1631-0705/$ – see front matter
http://dx.doi.org/10.1016/j.crhy.2013.02.003

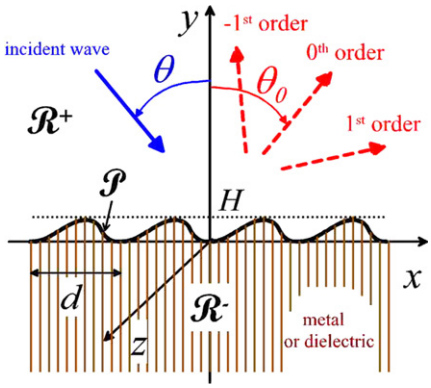

Fig. 1. Notations.

extraordinary transmission through subwavelength hole arrays [2] or the use of surface plasmons to generate superlenses in nanophotonics [3,4].

Extreme absorption phenomena have led to very interesting practical applications. A very selective absorption in incidence and frequency ranges can be used in metrology or to make selective filters like biosensors or rejection filters. Since Wood's anomalies bring with them strong local enhancements of the field on the grating surface, they are used in Raman scattering or second-harmonic generation. On the other hand, wide-range absorption can be applied for making absorbers for solar energy or efficient photovoltaic cells [5].

The first part of the paper will be devoted to a quite surprising phenomenon, the most amazing in the domain of Wood's anomalies: the total absorption of light by a shallow metallic grating, discovered in 1976 [6,7]. The phenomenon will be shown from numerical calculations and experimental confirmations. Then, it will explained through a quantitative phenomenological theory of Wood's anomalies [8] based on the theory of analytic functions of complex variable. This theory was the first one to provide quantitative representations of the anomalies using a very simple phenomenological formula. In addition, it permitted the prediction of new phenomena. The numerical results given in this paper have been obtained from our original grating theory of metallic and dielectric gratings, the only one that leads to a single integral equation. A brief description of this theory will be given.

2. Notations, grating formula

2.1. Notations

The grating is represented in Fig. 1. It is made of a cylindrical (2D) surface $\mathscr{P}$ of period d separating the air (in region $\mathscr{R}^+$ located above the grating profile) from a metallic or dielectric non-magnetic material (in region $\mathscr{R}^-$ located below the grating profile) characterized by its complex optical index ν, the time dependence being in $\exp(-i\omega t)$. The bottom of $\mathscr{P}$ lies on the x-axis, while its top is located at ordinate H. The y-axis is orthogonal to the mean plane of the grating profile and the z-axis is the invariance axis of the structure. The grating profile is illuminated with an incidence angle θ (measured with anticlockwise convention from the y-axis) by a monochromatic plane wave of wavelength in the air $\lambda = 2\pi/k$ propagating in the xy-plane. Classically, two fundamental cases of polarization are distinguished, denoted by TE or TM, according to whether the electric or magnetic incident field is parallel to the z-axis. By convention, we will denote by F^i the component on the z-axis of the electric field $\vec{E^i}$ for TE polarization, or of the magnetic field $\vec{H^i}$ for TM polarization. Thus, the incident field can be written:

$$\vec{F^i} = \hat{z}\exp(ikx\sin\theta - iky\cos\theta) \tag{1}$$

with $\hat{z}$ being the unit vector of the z-axis. Here, we assume that the incident field has an amplitude equal to unity.

2.2. The boundary-value problem

The grating problem is to find the total field F generated by the grating. In order to solve it rigorously or to establish analytic properties, it is necessary to reduce the physical problem to a mathematical problem. With this aim, let us state two intuitive properties of the field. First, let us notice that the physical problem remains unchanged after translations of the grating or of the incident wave along the z-axis, since both do not depend on z. Therefore, if $\vec{F}(x, y, z)$ is the total field, $\vec{F}(x, y, z + z_0)$ will a solution too, regardless of the value of z_0. Assuming, by physical intuition, that the solution of the grating problem is unique, we deduce that $\vec{F}$ is independent of z, like the incident field $\vec{F^i}$. This property shows that the grating problem is two-dimensional. Using similar arguments, it can be shown that the total field F remains parallel to the z-axis, thus $\vec{F}(x, y) = F(x, y)\hat{z}$. Now, we must define the diffracted field F^d:

$$\overrightarrow{F^d} = \begin{cases} \vec{F} - \overrightarrow{F^i} & \text{in } \mathscr{R}^+ \\ \vec{F} & \text{in } \mathscr{R}^- \end{cases} \tag{2}$$

It is easy, by combining the first two Maxwell equations, to show that the total and scattered fields satisfy a Helmholtz equation:

$$\nabla^2 F^d(x, y) + k^2 \varepsilon(x, y) F^d(x, y) = 0 \tag{3}$$

with relative permittivity $\varepsilon(x, y)$ being a piecewise constant function:

$$\varepsilon(x, y) = \begin{cases} 1 & \text{in } \mathscr{R}^+ \\ \nu^2 & \text{in } \mathscr{R}^- \end{cases} \tag{4}$$

In order to state the boundary-value problem, it is necessary to add a second requirement: the scattered field must satisfy two boundary conditions on $\mathscr{P}$, deduced from the continuity of the tangential components of $\vec{E}$ and $\vec{H}$. Using Maxwell equations, these continuities lead to the following equations [9,10]:

$$\left[F^d\right]^- = \left[F^d\right]^+ + \left[F^i\right]^+ \tag{5}$$

$$\left[\frac{\mathrm{d}F^d}{\mathrm{d}n}\right]^- = C\left\{\left[\frac{\mathrm{d}F^d}{\mathrm{d}n}\right]^+ + \left[\frac{\mathrm{d}F^i}{\mathrm{d}n}\right]^+\right\} \tag{6}$$

$$C = \begin{cases} 1 & \text{for TE polarization} \\ \nu^2 & \text{for TM polarization} \end{cases} \tag{7}$$

with the symbol $[u]^{\pm}$ denoting the limit of u on the profile $\mathscr{P}$ in $\mathscr{R}^{\pm}$.

Finally, the third condition of the boundary-value problem is that the diffracted field must satisfy a radiation condition (or Sommerfeld condition, or outgoing wave condition) at infinity, in contrast with the total field, which does not satisfy this condition in $\mathscr{R}^+$. This means that the diffracted field must remain bounded and propagate upwards in $\mathscr{R}^+$ when $y \to +\infty$, whereas it must remain bounded and propagate downwards in $\mathscr{R}^-$ when $y \to -\infty$. It can be shown that the solution of this boundary-value problem exists and is unique.

2.3. Pseudo-periodicity of the field and grating formula

The demonstration of the property of pseudo-periodicity evidences the vital importance of the theorem of existence and uniqueness of the solution of the boundary-value problem, which could seem useless for the physicist at first glance. It is straightforward to show that the function $G(x, y) = F^d(x + d, y)\exp(-i\alpha d)$, with $\alpha = k\sin(\theta)$, satisfies all the conditions of the boundary-value problem. Thus, due to the uniqueness, $G(x, y) = F^d(x, y)$, which entails that:

$$F^d(x + d, y) = F^d(x, y)\exp(\mathrm{i}\alpha d) \tag{8}$$

This property of pseudo-periodicity becomes obvious in the case of normal incidence ($\theta = 90°$) in which the pseudo-periodicity reduces to a simple periodicity of the field. From the pseudo-periodicity, it can be derived that $F^d(x, y)\exp(-i\alpha x)$ is periodic and can be expanded in Fourier series:

$$F^d(x, y)\exp(-i\alpha x) = \sum_{n=-\infty}^{+\infty} F_n^d(y)\exp(2\mathrm{i}\pi n x/d) \tag{9}$$

Inserting the value of $F^d(x, y)$ deduced from Eq. (9) in the Helmholtz equation (Eq. (3)), bearing in mind that the Fourier coefficients vanish if the Fourier series vanishes for any value of x, it turns out that $F_n^d(y)$ is a sum of exponential functions outside the intermediate region $0 < y < H$. It is not so in the intermediate region, since $\varepsilon(x, y)$ is not constant for a given value of y. After straightforward calculations and taking into account the radiation condition, it can be derived that:

$$F^d(x, y) = \begin{cases} \sum_{n=-\infty}^{+\infty} r_n \exp(\mathrm{i}\alpha_n x + \mathrm{i}\beta_n y) & \text{if } y > H \\ \sum_{n=-\infty}^{+\infty} t_n \exp(\mathrm{i}\alpha_n x - \mathrm{i}\gamma_n y) & \text{if } y < 0 \end{cases} \tag{10}$$

$$\alpha_n = \alpha + 2\pi n/d \tag{11}$$

$$\beta_n = \left(k^2 - \alpha_n^2\right)^{1/2}, \qquad \gamma_n = \left(k^2\nu^2 - \alpha_n^2\right)^{1/2} \tag{12}$$

$$\mathrm{Re}(\beta_n) + \mathrm{Im}(\beta_n) > 0, \qquad \mathrm{Re}(\gamma_n) + \mathrm{Im}(\gamma_n) > 0 \tag{13}$$

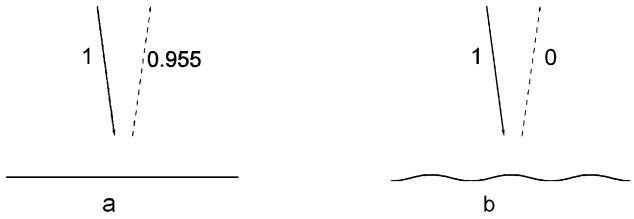

Fig. 2. (a) Reflection by a gold mirror. (b) Reflection by a shallow gold grating (scale picture of the profile).

It can be verified that the last equation imposes the field given by Eq. (10) to satisfy the radiation condition (it is straightforward if β_n and γ_n are purely real or imaginary). The conclusion of this subsection is that above and below the intermediate region, the field reflected and transmitted by the grating takes the form of sums of plane waves, each of them being characterized by its order.

It must be emphasized that the validity of the plane wave expansion does not extend to the intermediate region. The hypothesis of its validity was made by Rayleigh [11,9,10]. Of course, this hypothesis considerably simplifies the grating problem: it suffices to match the two plane wave expansions on the profile $\mathscr{P}$ using the boundary conditions on the profile. This question has raised endless controversies that are not closed nowadays! The interested reader can find reviews on this subtle subject in [9,10].

According to Eq. (12), almost all the diffracted plane waves in $\mathscr{R}^+$ (an infinite number) are evanescent: they propagate along the x-axis at the vicinity of the grating profile, since they decrease exponentially when $|y| \to +\infty$. They correspond to the orders n such that $\alpha_n^2 \geqslant k^2$, thus rendering β_n a purely imaginary number. Only a finite number of them, called y-propagative orders, propagate towards $y = +\infty$, with $\alpha_n^2 \leqslant k^2$, thus β_n being real. Let us notice that among these orders, the 0th order is always included, since $\beta_0 = k\cos\theta$. It propagates in the direction specularly reflected by the mean plane of the profile, whatever the wavelength may be. In contrast, the other y-propagative orders are dispersive. Indeed, their propagation constants along the x- and y-axes are equal to α_n and β_n, in such a way that the diffraction angle θ_n of one of these waves, measured clockwise from the y-axis, can be deduced from $\alpha_n = k\sin\theta_n$. Using the expression of α_n given by Eq. (11), the angle of diffraction is given by:

$$\sin\theta_n = \sin\theta + n\frac{2\pi}{kd} = \sin\theta + n\frac{\lambda}{d} \tag{14}$$

This is the famous grating formula, often deduced from heuristic arguments of physical optics. When the material inside $\mathscr{R}^-$ is lossless, another grating formula can be stated for transmitted waves. Otherwise, the field decreases exponentially when $y \to -\infty$.

Using the Poynting theorem, it can be shown that the efficiency ρ_n of the grating in a given non-evanescent reflected order n (viz. the part of the incident energy that is scattered in this order) is given from the amplitude r_n by $\rho_n = \frac{\beta_n}{\beta_0}|r_n|^2$.

3. Total absorption of light by a diffraction grating

The phenomena of strong absorption provoked by Wood's anomalies is one of the origins of the large interest raised by gratings in nanotechnology, especially in plasmonics. Grating anomalies were discovered experimentally by Wood at the beginning of the twentieth century [1]. R.W. Wood, observing the spectrum of a continuous light source given by an optical metallic diffraction grating, noticed a surprising phenomenon: "I was astounded to find that under certain conditions, the drop from maximum illumination to minimum, a drop certainly of from 10 to 1, occurred within a range of wavelengths not greater than the distance between the sodium lines". Wood made a crucial remark: these lines were present only for TM polarized light. However, he was unable to provide any interpretation to these phenomena and thus termed them 'singular anomalies', concluding that this problem was 'one of the most interesting that I have ever met with'. Grating anomalies have fascinated specialists of optics for more than one century. Long after the first interpretation given by Lord Rayleigh, U. Fano [12] has suggested that the origin of anomalies could be found in the excitation of surface waves. This chapter describes the quantitative phenomenological theory of Wood's anomalies developed in the 1970s [6,8], using as a starting point the heuristic interpretation given by Fano, then the macroscopic laws of electromagnetics, the theory of analytic functions of the complex variable and finally numerical computations. This theory leads to a formula giving the efficiency of gratings in the region of anomaly, which predicts the phenomenon of total absorption of light by a grating [8].

3.1. Numerical evidence of total absorption

3.1.1. The phenomenon in outline

Fig. 2 outlines a quite surprising phenomenon. A TM polarized incident light with wavelength 647 nm illuminates a 1800 grooves/mm gold sinusoidal diffraction grating having a width $H = 40$ nm. The period d of the grating being equal to 555.5 nm, the ratio $H/d = 40/555.5$ is equal to 0.072, thus this grating can be considered as very shallow. Fig. 2 (right side) shows a picture at scale of the profile. It is worth noting that a perfectly plane surface illuminated with the same

incidence has a reflectance of 95.5%. Nevertheless, the grating does not scatter any plane wave at infinity! All the incident energy is absorbed by Joule effect in the metal. It must be emphasized that this is not a simple phenomenon of very strong absorption. As we will see further, it is an absolute total absorption, at least from a theoretical point of view.

3.1.2. The rigorous theory of scattering by diffraction gratings

The numerical results given in the following have been obtained using an original theory of gratings. At the beginning of the 1970s, the problem of scattering by diffraction gratings was solved for perfectly conducting gratings, and for some kinds of grating profiles only. Indeed, it was considered in general that, considering the high reflectance of metals in the visible region, the approximation of perfect conductivity was justified. However, some attempts at solving the problem of metallic and dielectric gratings were achieved (see for example [13]). In contrast with the theory of perfectly conducting gratings, which leads to a single integral equation, the classical theory dealing with finitely conducting gratings leads to a set of two integral equations with two unknown functions. This feature makes a big difference in the numerical implementation. A set of two coupled integral equations requires much larger memory storage and time computation. This explains why very few numerical results were published, all these results dealing with lossless dielectric gratings. Due to the development of space optics (with gratings used in the ultraviolet region) and the beginning of the production of holographic gratings, it was necessary to eleborate an accurate theoretical and numerical tool to predict the properties of gratings of any profile and any conductivity in the entire range of wavelengths, from X-rays to microwaves. This theory was published in 1972 [14,15]. The first numerical results on metallic gratings demonstrated an unexpected result: the inadequacy of the theory of perfectly conducting gratings in the ultraviolet, visible, and near-infrared regions!

The success of this formalism was based on two basic properties of the theory. First, of course, this theory leaded to a single integral equation. Secondly, a meticulous attention was devoted to numerical analysis, specially to the summation and integration of the kernel of the integral equation, especially in the very difficult case of metallic gratings in which some elements of the kernel are close to delta distributions. Let us briefly outline the theory. The classical theory of finitely conducting gratings is based on the second Green's theorem. Using this theorem, it is possible to express in an integral form the scattered field in $\mathscr{R}^+$ or $\mathscr{R}^-$ from two unknown functions: the limits of the field and its normal derivative above the profile (for $\mathscr{R}^+$) or below (for $\mathscr{R}^-$). Since these limits above and below the surface are linked by the two boundary conditions on the profile (Eqs. (5) and (6)), it turns out that the field at any point of space can be expressed in an integral form from two unknown functions only using the second Green's theorem. Of course, two integral equations are needed to determine these two unknown functions. Unfortunately, these two equations are coupled.

The new theory demonstrated that in fact, the two unknown functions in the classical theory can be derived from a single one and that it exists in some way a redundancy in the classical theory. Considering the case of TE polarization, a heuristic presentation of the new theory can be given. Replacing the metal by air, the new theory has demonstrated that it exists one, and only one distribution of surface current density that, placed on the grating profile (with air above and below), generates in $\mathscr{R}^+$ the actual scattered field in the real problem of scattering. It is easy to understand that this fictitious surface current density allows one to express the field in $\mathscr{R}^+$. Indeed, a surface current density is nothing else that the limit of a finite set of line currents located in the air on discrete points of the profile, the number of discrete points tending to infinity and the distance between two adjacent points to zero. From this expression of the field in $\mathscr{R}^+$, the limits of the field and its normal derivative above the profile can be deduced, then the limits below the profile using the two boundary conditions, then the field below the profile using the second Green's theorem. The field at any point of space being expressed from a single function, a single integral equation is needed to find it.

This theory has been the starting point of numerous theoretical and numerical studies achieved by mathematicians or specialists of theoretical physics (see, for example, [16,17]), in such a way that this theory has been generalized to many other scattering problems, including three-dimensional and time-depending ones. Since more than 20 years, the software 'RESEAU 2000' elaborated from this theory is used in about 20 academic and industrial scientific centers throughout the world. For example, it has allowed the optimization of gratings used in about 40 space and terrestrial projects of astronomy, the realization of sophisticated nearly lossless metallic gratings used as beam samplers for high power lasers, as well as the choice of selective gratings for optical multiplexing.

3.1.3. Numerical and experimental verifications

Let us give the numerical and experimental results that proved the existence of this phenomenon. It was discovered from a phenomenological approach [6], then confirmed by numerical and experimental data. Before the phenomenological theory, we will provide the numerical and experimental proofs of total absorption.

After a first numerical verification [6], a wide study [7] provided detailed numerical and experimental verifications of total absorption. These numerical data were obtained from our theory of gratings [14,15].

The theoretical parameters of the totally absorbing grating were previously given in Section 3.1. The experimental data were performed on a holographic sinusoidal gold grating having the same period (555.5 nm), illuminated by a krypton laser beam at the wavelength 647 nm. Due to a mishap during exposure, the groove width varied from 13 nm on one side to 75 nm on the other. For studying the reflectance as a function of the groove width, it was necessary simply to select the appropriate region of the grating surface. The groove depth was measured using a profilometer fitted with a chisel-shaped stylus. The results are given in Fig. 3. The agreement between experimental and theoretical results is excellent. The minimum reflectance of 0.3% of the holographic grating was at an angle of incidence of 6.6° and a groove depth of

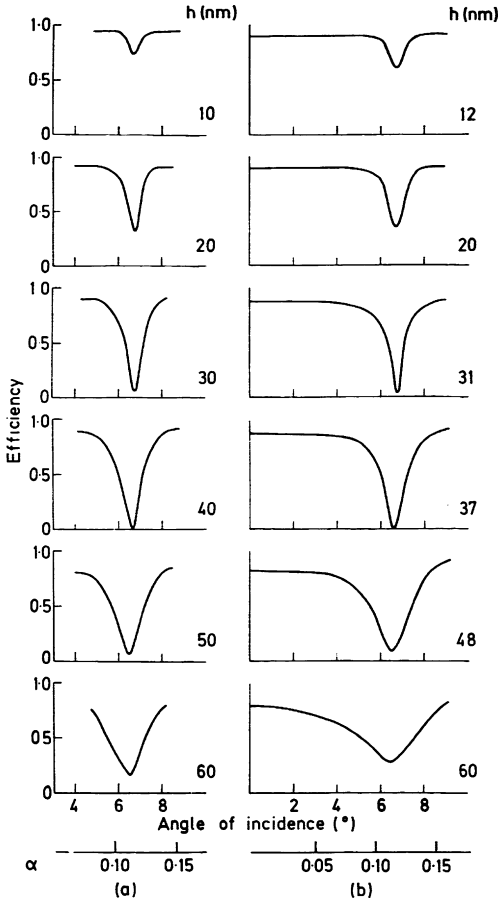

Fig. 3. Theoretical (a) and experimental (b) efficiency curves for gratings versus the incidence angle, for various groove depths. Reprinted from M.C. Hutley and D. Maystre, The total absorption of light by a diffraction grating, Opt. Commun. 19 (1976) 431–436, with permission from Elsevier.

37 nm, which are very close to the theoretical predictions. This result is quite remarkable and very surprising: a very gentle modulation in the surface of a gold mirror causes the reflectance to fall dramatically from over 95% to below 1%. Fig. 3 also shows that the width of the reflectance drop is very small, of the order of 1°. The resonance remains very selective when other parameters (wavelength, groove depth) are changed. Outside the resonance region, the reflectance rapidly reaches a value close to the reflectance of the plane metallic surface.

4. Phenomenological theory of Wood's anomalies

4.1. Surface plasmon resonance on a flat surface

In this section, we consider a different, but closely related problem: the problem of guiding. The question is to know whether a surface wave can propagate at the surface of the metal. The answer to this question requires a precise definition of a guided wave. Classically, a guided wave is a wave propagating along the x-axis and satisfying a radiation condition at infinity on both sides of the plane interface. Assuming the plane interface to lay on the xz-plane and denoting by $\hat{\alpha}$ the propagation constant along the x-axis of the guided wave, the field $F(x, y)$ of this guided wave can be written in the form:

$$F(x, y) = \eta(y) \exp(\mathrm{i}\hat{\alpha}x) \tag{15}$$

Following the same lines as in Section 2.3, it turns out by inserting Eq. (15) in the Maxwell equations and using the radiation condition that $\eta(y)$ takes the form of exponentials. Taking into account the radiation condition yields:

$$F(x, y) = \begin{cases} a \exp(\mathrm{i}\hat{\alpha}x + \mathrm{i}\hat{\beta}y) & \text{if } y > 0 \\ b \exp(\mathrm{i}\hat{\alpha}x - \mathrm{i}\hat{\gamma}y) & \text{if } y < 0 \end{cases} \tag{16}$$

$$\hat{\beta} = \left(k^2 - \hat{\alpha}^2\right)^{1/2}, \qquad \hat{\gamma} = \left(k^2\nu^2 - \hat{\alpha}^2\right)^{1/2} \tag{17}$$

$$\mathrm{Re}(\hat{\beta}) + \mathrm{Im}(\hat{\beta}) > 0, \qquad \mathrm{Re}(\hat{\gamma}) + \mathrm{Im}(\hat{\gamma}) > 0 \tag{18}$$

Such a guided wave must satisfy the boundary conditions stated in Eqs. (5) and (6), cancelling the incident field in these equations, since it vanishes in a guided wave. Inserting the expression of the guided wave given by Eq. (16) in these boundary conditions leads to a homogeneous system of two linear equations with the two unknowns a and b. The compatibility condition imposes the determinant of this system to vanish. After some elementary calculations, it emerges that no solution exists for TE polarization, whereas for TM polarization, the solution is given by:

$$\hat{\alpha} = \frac{\pm k\nu}{(1+\nu^2)^{1/2}}, \qquad \hat{\beta} = \frac{-k}{(1+\nu^2)^{1/2}}, \qquad \hat{\gamma} = \frac{k\nu^2}{(1+\nu^2)^{1/2}} \tag{19}$$

The two opposite values of $\hat{\alpha}$ given by Eq. (19) represent the constants of propagation of two identical waves, but propagating in opposite directions.

In solid-state physics, this guided wave is called SPP (surface plasmon polariton) and is attributed to a collective resonance of the electrons on the metal surface [18]. The first quantitative electromagnetic studies on Wood's anomalies published in the 1970s had to face controversial criticisms: a theory that does not include the basic laws of electron motion should not provide a reliable description of SPP. Nowadays, this controversy is closed: the SPP is a macroscopic property of electrons and a macroscopic property is fully represented by the optical index of metal.

It is worth noting that $\hat{\alpha}$ has a small positive imaginary part in the visible, near-ultraviolet and infrared regions for usual metals (Al, Au, Ag, for example). For example, for aluminium at 647 nm, the optical index is equal to $1.3 + \mathrm{i} \times 7.1$ and $\hat{\alpha} = k(1.019 + \mathrm{i} \times 7.6 \times 10^{-3})$. This property is rather intuitive. Indeed, due to the losses inside the metal, the energy of the SPP decreases during propagation, which entails a decreasing exponential term in $\exp(\mathrm{i}\hat{\alpha}x)$. Nevertheless, in this example, the SPP can propagate on a distance of 20 wavelengths with an attenuation by a factor of 3 only, a result quite important for the use of SPP as waveguides in nanophotonics. Moreover, the value of $\mathrm{Re}(\hat{\alpha})$ is slightly greater than k in modulus. As a consequence, the SPP cannot be excited by a plane wave: the propagation constant $k\sin\theta$ of an incident plane wave along the x-axis is always smaller than k, and thus it cannot match $\mathrm{Re}(\hat{\alpha})$. The next subsection will show that this remark does not hold any more when the metal surface is periodically modulated.

4.2. Surface plasmon resonance on a diffraction grating

As in the case of a flat surface we search for a solution of a wave satisfying a radiation condition at infinity. The vital consequence of a periodic modulation of the metal surface is that the constant of propagation $k\hat{\alpha}$ becomes a series of propagation constants $\hat{\alpha}_n$, according to the Floquet–Bloch theorem, with:

$$\hat{\alpha}_n = \hat{\alpha}_0 + 2\pi n/d \tag{20}$$

The expression of the SPP is now given by a series:

$$F(x,y) = \begin{cases} \sum_{n=-\infty}^{+\infty} a_n \exp(\mathrm{i}\hat{\alpha}_n x + \mathrm{i}\hat{\beta}_n y) & \text{if } y > H \\ \sum_{n=-\infty}^{+\infty} b_n \exp(\mathrm{i}\hat{\alpha}_n x - \mathrm{i}\hat{\gamma}_n y) & \text{if } y < 0 \end{cases} \tag{21}$$

$$\hat{\beta}_n = \left(k^2 - \hat{\alpha}_n^2\right)^{1/2}, \qquad \hat{\gamma}_n = \left(k^2\nu^2 - \hat{\alpha}_n^2\right)^{1/2} \tag{22}$$

$$\mathrm{Re}(\hat{\beta}_n) + \mathrm{Im}(\hat{\beta}_n) > 0, \qquad \mathrm{Re}(\hat{\gamma}_n) + \mathrm{Im}(\hat{\gamma}_n) > 0 \tag{23}$$

It must be noticed that the numbering of the parameters in Eq. (21) is ambiguous, since changing n into $n+p$ (p constant integer) does not modify the sum of the series. In order to fix this determination, we can notice that one of the terms of the series must tend to the SPP of the plane when the width H of the grating tends to zero. For example, if the profile is sinusoidal, we can go continuously from the grating to the plane by decreasing H. By definition, the term of the series corresponding to the SPP of the flat surface is numbered by 0. Thus, it turns out that, by convention:

$$\lim_{H\to 0} \hat{\alpha}_0 = \hat{\alpha} \tag{24}$$

Fig. 4 shows the locations of the constants of propagation in the complex plane. The different components of the SPP represented in Fig. 4 are very different in nature. Bearing in mind that the imaginary part of the propagation constants $\hat{\alpha}_n$ is very small (at least if the width of the grating is not large), the nth term $a_n \exp(\mathrm{i}\hat{\alpha}_n x + \mathrm{i}\hat{\beta}_n y)$ of the grating SPP in the air is very close to a plane wave propagating upwards if $-k < \mathrm{Re}(\hat{\alpha}_n) < +k$ (the orders located between the two vertical dashed lines in Fig. 4, namely the -1st and -2nd orders, classified as 'leaky waves'), whereas all the other ones are very close to evanescent waves. As a consequence, the far field includes these two orders only, as shown in Fig. 5. In contrast with the SPP of a plane interface, that of a grating includes waves carrying energy at infinity. These waves generate supplementary losses during propagation; thus it can be expected that the imaginary part of the propagation constants of the grating is greater than that of the plane interface.

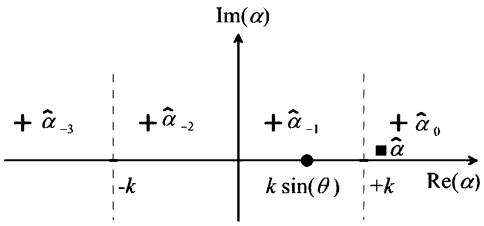

Fig. 4. Location of the propagation constants of the plane interface (black square) and of the grating (crosses) in the complex plane. The propagation constant $\hat{\alpha}_0$ of the grating SPP tends to that of the plane $\hat{\alpha}$ as the width of the grating tends to 0. The black circle represents the propagation constant of an incident plane wave along the x-axis.

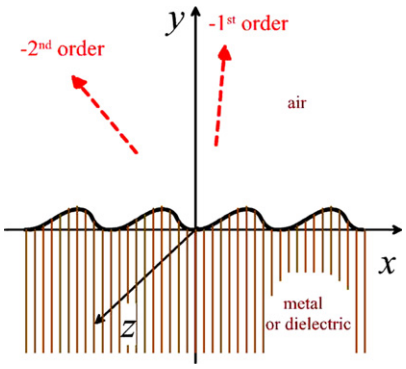

Fig. 5. Far field generated by the SPP.

4.3. *Phenomenological formula, total absorption*

Until now, we have described qualitatively the scattering and guiding properties of gratings. The aim of this section is to deduce from these heuristic considerations quantitative predictions on Wood's anomalies [8]. With this aim, our tool is the theory of analytic functions of the complex variable.

4.3.1. *Poles and zeros of the leaky waves*

First, let us compare Fig. 1, which schematizes the scattering properties of gratings, and Fig. 5, which represents its guiding properties. At first glance, the conclusion that can be drawn from this comparison is that the SPP is nothing else than the field in a problem of scattering (red dashed arrows in Fig. 1) but without any incident wave (blue solid arrow in Fig. 1). From a mathematical point of view, it is equivalent to state that the scattered field in the physical scattering problem (Fig. 1) may be infinite, provided that the propagation constant $\alpha = k\sin\theta$ of the incident plane wave is allowed to include an imaginary part. Of course, this incident plane wave must have adequate characteristics, in order to generate the scattered waves represented by red dashed arrows in Fig. 5. This aim is reached if the propagation constant along the x-axis of the incident wave is the same as that of one of the leaky waves in Fig. 5, the propagation constant along the y-axis being the opposite. It can be deduced that two solutions exist, the two incident plane waves being given by $F^{\mathrm{i}} = \exp(\mathrm{i}\hat{\alpha}_{-1}x - \mathrm{i}\hat{\beta}_{-1}y)$ and $F^{\mathrm{i}} = \exp(\mathrm{i}\hat{\alpha}_{-2}x - \mathrm{i}\hat{\beta}_{-2}y)$. Mathematically, it can be deduced from this property that $\hat{\alpha}_{-1}$ and $\hat{\alpha}_{-2}$ are poles of all the amplitudes r_n and t_n of the scattered field above and below the grating surface, including the evanescent waves (see Eq. (10)).

It seems that this remark is useless, since $\alpha = k\sin(\theta)$ is real, while $\hat{\alpha}_{-1}$ and $\hat{\alpha}_{-2}$ are complex (Fig. 4), thus the corresponding incident waves cannot be realized in the real life. However, these poles have a vital importance on grating properties. Indeed, it can be considered that in the real life, the amplitudes r_n and t_n are complex functions of the real variable α, constant of propagation of the incident wave along the x-axis. Mathematical theorems [19] state that a complex function of the real variable α has one and only one analytic continuation in the complex plane of α. It turns out that $\hat{\alpha}_{-1}$ and $\hat{\alpha}_{-2}$ are the poles of the continuations of the scattering amplitudes. The effect on the real axis (the real life…) of these poles is all the more crucial since their imaginary part is very small. Classically, the analytic continuations are not distinguished from the functions of the real variable.

In order to simplify, we assume in the following that, in contrast with the situation in Fig. 4, the only order n for which $-k < \mathrm{Re}\,\hat{\alpha}_n < +k$ is the -1st order. Let us notice that it is easy to satisfy this condition, according to Eq. (20), by decreasing the period of the grating in order to move $\hat{\alpha}_{-2}$ to the left of the left vertical dashed line in Fig. 4. In that case, the pole of all the scattered amplitudes is unique and equal to $\hat{\alpha}_{-1}$. In the following, we will denote by α^p this pole: $\alpha^p = \hat{\alpha}_{-1}$. Finally, according to Eq. (20),

$$\alpha^p = \hat{\alpha}_0 - 2\pi/d \approx \hat{\alpha} - 2\pi/d \tag{25}$$

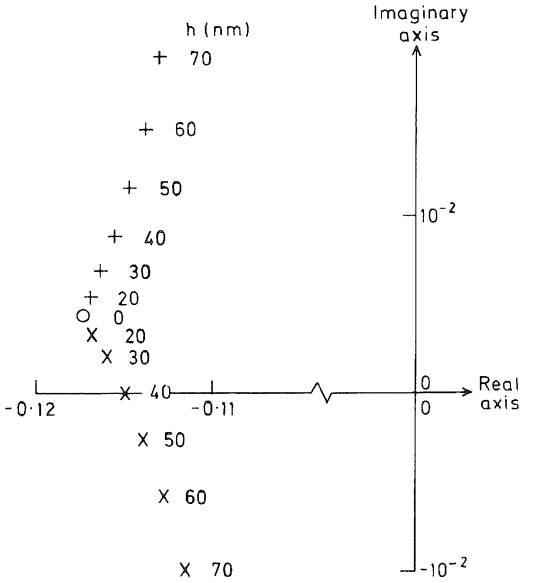

Fig. 6. Trajectories of the pole and zero in the complex plane of $\sin\theta = \alpha/k$. The parameters of the grating are those given in Section 3.1: the 1800 grooves/mm (period 555.5 nm) gold sinusoidal diffraction grating is illuminated by a TM polarized incident light with wavelength 647 nm.

If the incidence θ is chosen in such a way that the real variable $\alpha = k\sin\theta$ is close to $\mathrm{Re}(\alpha^p)$, we can expect a rapid variation of the amplitude of all the scattered orders, and specially of the 0th order, which is the only non-evanescent order according to our hypothesis.

Now, we establish the mathematical consequences of this heuristic remark. Assuming that the amplitudes do not present any other singularity in the vicinity of α^p, they can be expanded in a Laurent series. For the 0th order, we obtain:

$$r_0 = \frac{c_{-1}}{\alpha - \alpha^p} + c_0 + c_1(\alpha - \alpha^p) + c_2(\alpha - \alpha^p)^2 + \cdots \tag{26}$$

Neglecting the terms of order $n > 0$, this equation can be written in the form:

$$r_0 \approx c_0 \frac{\alpha - \alpha^z}{\alpha - \alpha^p} \tag{27}$$

$$\text{with} \quad \alpha^z = \alpha^p - \frac{c_{-1}}{c_{-0}} \tag{28}$$

The amplitude of the unique non-evanescent scattered order has been expressed from three complex numbers, the pole α^p, the zero α^z and the constant c_0. If the width of the grating tends to 0, there is no more resonance and then, c_{-1} tends to 0. Thus, from Eq. (28), α^z tends to α^p: the effects of the pole and zero annihilate and the coefficient c_0 tends to the reflection coefficient r of a flat metallic plane. Assuming that c_0 remains close to this reflectivity, at least if the width of the grating is not large, yields the phenomenological formula:

$$r_0 \approx r \frac{\alpha - \alpha^z}{\alpha - \alpha^p} \tag{29}$$

Thus the efficiency in the zeroth order is given by:

$$\rho_0 \approx R \left| \frac{\alpha - \alpha^z}{\alpha - \alpha^p} \right|^2 \tag{30}$$

with R being the reflectance of the metallic plane.

In order to compute the locations of poles and zeros in the complex plane, we adapted our integral theory of gratings to complex values of $\alpha = k\sin\theta$. Two ways can be used to reach this aim, by complexifying either the wavelength or the incidence. As in most numerical studies, we consider in the following that the incidence (thus α) is complex. Moreover, we have elaborated a subroutine able to locate the zero of a complex function of a complex variable. This software, based on simple mathematics (it is a straightforward extension of Newton's formula for finding the root of a real function of the real variable) requires an estimate of the location of the zero (or of the pole, which is nothing else than the zero of the inverse function). Our estimate is given by Eq. (25). Fig. 6 shows the computed trajectories of the pole and zero for a sinusoidal

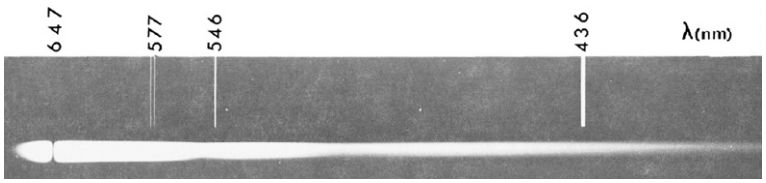

Fig. 7. Spectrum of a white light beam after reflection from the gold grating of Fig. 2 with groove width 37 nm and incidence 6.6°. Reprinted from M.C. Hutley and D. Maystre, The total absorption of light by a diffraction grating, Opt. Commun. 19 (1976) 431–436, with permission from Elsevier.

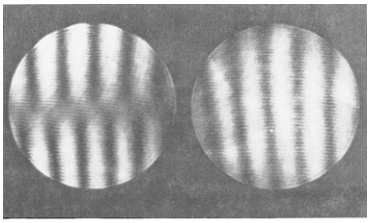

Fig. 8. Interferogram, made using a Mach–Zender interferograph, of the wavefront reflected by a grating with non-uniform groove height: (a) TM polarization, (b) TE polarization. Reprinted from M.C. Hutley and D. Maystre, The total absorption of light by a diffraction grating, Opt. Commun. 19 (1976) 431–436, with permission from Elsevier.

grating when the width of the grating is increased. When the width of the grating increases, the imaginary part of the pole is increased, while the zero moves to the real axis and finally crosses this axis for $H = 40$ nm.

The precision of the phenomenological formula has been checked by comparing the numerical curves of Fig. 3 (left) to theoretical curves deduced from Eq. (30). To this end, we included in this equation the computed values of α^z and α^p (see Fig. 6). The discrepancy remains smaller than 10^{-2} in absolute value, in such a way that all the numerical efficiency curves of Fig. 3 cannot be distinguished from those deduced from the phenomenological formula. This result evidences the remarkable accuracy of the phenomenological formula in the region of anomaly. It confirms the strong power of phenomenological approaches, which reduce complex phenomena to the knowledge of few parameters. Unfortunately, these approaches are more and more ignored in the field of electromagnetics and electromagnetic optics, at least for two reasons: they require deep (and sometimes long!) thoughts about the physical origin of the phenomena and in general, they use non-straightforward tools of applied mathematics (here the theory of analytic functions). This section also showed that the first interpretation of Wood's anomalies given by Rayleigh [20], viz. the passing-off of a y-propagating order, is not correct, even though it leads to acceptable predictions of the location of anomalies, due to the fact that $\mathrm{Re}(\hat{\alpha}_0)$ is close to k. In the next section, we show that our approach allows one to predict the main characteristics of the anomalies in closed form.

4.4. Total absorption

When the trajectory of the zero crosses the real axis in Fig. 6, the zero becomes real and comes to the real life. The amplitude of the zeroth order vanishes if $k \sin\theta = \alpha^z$. Since this order is the only scattered order, there is not any scattered field at infinity: the incident energy is entirely lost by Joule effect. This conclusion may be criticized since Eq. (29) is approximate. In fact, it is easy to show that a rigorous equation can be stated by replacing the constant r by a slowly varying function $f(\alpha)$, thus the phenomenon is actually a phenomenon of total absorption, at least from a theoretical point of view. The phenomenological formula also provides valuable information on the anomalies. For example, assuming that the real parts of the pole and zero are very close to each other (that is the case in general), the minimum value $\rho_0^{\min}$ of the efficiency and the width w at half-width of the drop of efficiency are given by:

$$\rho_0^{\min} \approx R \left| \frac{\mathrm{Im}(\alpha^z)}{\mathrm{Im}(\alpha^p)} \right|^2 \tag{31}$$

$$w \approx 2\,\mathrm{Im}\left(\alpha^p\right) \tag{32}$$

From Fig. 6, it turns out that $\mathrm{Im}(\alpha^p)$ strongly increases with H, thus w increases and the absorption becomes smaller and less selective.

It has been shown from numerous theoretical and numerical analyses that for a given shape (sinusoidal, triangular…) and a given period of the grating profile, with given metal and incidence angle, a phenomenon of total absorption occurs for TM polarized light for adequate wavelengths and groove depths, these two parameters depending on each other. Fig. 7 shows a spectrum of a polychromatic light scattered in the zeroth order by the grating of Fig. 2. The interferogram shown in Fig. 8 shows the shift of π of the amplitude r_0 scattered by the grating with groove width varying from 13 nm on one side to 75 nm on the other (see Section 3.1.3), when the groove width corresponds to total absorption, according to Eq. (29).

4.5. Applications

4.5.1. Generalizations

Further, the same phenomenological theory permitted the discovery of total absorption phenomena by metallic, dielectric coated gratings, for both polarizations. In that case, the SPP is replaced for TE polarization by the lossy guided waves propagating in the dielectric layer [21]. Comparable phenomenological theories have been developed to investigate the filtering properties of entirely dielectric gratings made of a dielectric waveguide laying on a dielectric substrate. It led to the optimization of highly selective DWDM (dense wavelength division multiplexing) instruments for optical communications [22]. It is worth noting that the study of anomalies has been generalized to the case in which the grating scatters more than a single order [8]. The phenomenon of total absorption by metallic gratings has been extended to unpolarized light using a crossed grating, viz. a grating having two orthogonal axes of periodicity [23]. More recently, N. Bonod et al. have demonstrated numerically that classical lamellar gratings (instead of crossed gratings) illuminated in conical (off-plane) mounting can achieve a total absorption of light for any polarization as well [24].

4.5.2. Localized surface plasmons

We have seen that the imaginary part of the pole strongly increases with the grating width. The first consequence is that the exponential decrease of surface plasmons during propagation becomes very strong, which explains why they are sometimes called localized plasmons. A second consequence is that very deep gratings generate non-selective absorptions in the visible and near-infrared regions [25]. A nearly total absorption on a wide range of incidence angles or wavelengths could lead to many practical applications. For example, this phenomenon has been employed for making efficient photovoltaic cells [5]. Other applications are the realization of solar absorbers [26] or light shielding of micro-photonic devices. As suggested by the Kirchhoff law, this kind of grating should constitute omnidirectional black-body emitters, possibly with narrow spectral range. A review of the applications of localized surface plasmons in many fields like optical transmission, information storage, nanophotonic devices, switches, resonant light scatterers (employed in the different near-field scanning optical microscopies), sensors and biosensors can be found in [27]. E. Popov et al. [28] have analyzed the behavior of another type of surface plasmons, which exists on deep-groove gratings, due to a standing wave resonance inside each groove, which is characterized by smaller absorption losses.

4.5.3. Various applications

Since Wood's anomalies entail strong local enhancements of the field on the grating surface, they are also used in Raman scattering [29] or second-harmonic generation [30]. E.L. Wood et al. showed that multiple-wavelength excitation of surface plasmons enables one to characterize a diffraction grating [31]. The propagation of surface plasmons entails the existence of bandgaps. These bandgaps may be used, for example for generating phenomena of Anderson localization of photons on the surface of random structures close to gratings [32]. W.L. Barnes et al. found grating profiles suitable for blocking surface mode propagation in all directions [33]. E.A. Smith and R.M. Corn used surface plasmon propagation to monitor biomolecular interactions using an array-based format [34].

4.5.4. A surprising application: virus detection

Finally, one of the most surprising applications of total absorption of light was the realization of immunosensors for virus detection (especially HIV). A direct immunosensor possesses the ability to observe antibody–antigen binding events in real time. An immunosensor can be made using the sensitivity of SPP to changes in the dielectric permittivity of a dielectric coated metallic grating [35]. It consists of a gold or silver holographic diffraction grating on which 'sensitizing' immunological molecules have been immobilized, realizing in some way a dielectric coating. If this coated grating realizes a total or quasi-total absorption, the subsequent binding of complementary components (possibly contained for example in human or animal serums deposited on the grating) results in a strong increase of the grating reflectivity. This technique was used for example in Africa for the rapid detection of HIV.

5. Conclusion

A quantitative phenomenological theory of Wood's anomalies based on the elementary laws of electromagnetics allowed us to predict the phenomenon of total absorption of light by metallic gratings: a very shallow periodic modulation of a metallic plane illuminated by a monochromatic light beam provokes a drop of the reflected intensity from more than 90% to zero. This phenomenon, confirmed by experimental measurements, has been used in many domains of science and technology. Nowadays, it constitutes one of the basic tools of plasmonics. It is worth noting that the phenomenological theory has been extended to randomly rough surfaces [36]. It allowed an electromagnetic explanation of the phenomenon of Anderson localization of photons and the definition of the new concept of 'localiton', a surface plasmon confined to a segment of a randomly rough surface.

References

[1] R.W. Wood, On a remarkable case of uneven distribution of light in a diffraction grating spectrum, Proc. Philos. Mag. 4 (1902) 396–402.

[2] T.W. Ebbesen, H.J. Lezec, H.F. Ghaemi, T. Thio, P.A. Wolff, Extraordinary optical transmission through subwavelength hole arrays, Nature 391 (1998) 667–669.
[3] J.B. Pendry, Negative refraction makes a perfect lens, Phys. Rev. Lett. 85 (2000) 3966–3969.
[4] D. Maystre, S. Enoch, Perfect lenses made with left-handed materials: Alice's mirror? J. Opt. Soc. Amer. A 21 (2004) 122–131.
[5] T.V. Teperik, F.J. Garcia de Abajo, A.G. Borisov, M. Abdelsalam, P.N. Bartlett, Y. Sugawara, J.J. Baumberg, Omnidirectional absorption in nanostructured metal surface, Nat. Photon. 2 (2008) 299–301.
[6] D. Maystre, R. Petit, Brewster incidence for metallic gratings, Opt. Commun. 17 (1976) 196–200.
[7] M.C. Hutley, D. Maystre, The total absorption of light by a diffraction grating, Opt. Commun. 19 (1976) 431–436.
[8] D. Maystre, General study of grating anomalies from electromagnetic surface modes, in: A.D. Boardman (Ed.), Electromagnetic Surface Modes, John Wiley and Sons Ltd., 1982 (Ch. 17).
[9] D. Maystre, Rigorous vector theories of diffraction gratings, in: E. Wolf (Ed.), Progress in Optics I, North-Holland, 1984.
[10] R. Petit (Ed.), Electromagnetic Theory of Gratings, Springer-Verlag, 1980.
[11] Lord Rayleigh, On the dynamical theory of gratings, Proc. Roy. Soc. A 79 (1907) 399–416.
[12] U. Fano, The theory of anomalous diffraction gratings and of quasi-stationary waves on metallic surfaces (Sommerfeld's waves), J. Opt. Soc. Amer. 31 (1941) 213–222.
[13] A. Neureuther, K. Zaki, Numerical methods for the analysis of scattering from non-planar periodic structures, Alta Freq. 38 (1969) 282–285.
[14] D. Maystre, Sur la diffraction d'une onde plane par un réseau métallique de conductivité finie, Opt. Commun. 6 (1972) 50–54.
[15] D. Maystre, A new general integral theory for dielectric coated gratings, J. Opt. Soc. Amer. 68 (1978) 490–495.
[16] R.E. Kleinman, P.A. Martin, On single integral equations for the transmission problem of acoustics, SIAM J. Appl. Math. 48 (1988) 307–325.
[17] E. Marx, Single integral equation for wave scattering, J. Math. Phys. 23 (1982) 1057–1065.
[18] H. Raether, Surface Plasmons on Smooth and Rough Surfaces and on Gratings, Springer Tracts in Modern Physics, vol. 111, Springer-Verlag, 1988.
[19] E.C. Titchmarsh, The Theory of Functions, 2nd edition, Oxford University Press, 1939.
[20] Lord Rayleigh, Note on the remarkable case of diffraction spectra described by Prof. Wood, Philos. Mag. 14 (1907) 60–65.
[21] E.G. Loewen, M. Nevière, Dielectric coated gratings – curious property, Appl. Opt. 16 (1977) 3009–3011.
[22] A.-L. Fehrembach, D. Maystre, A. Sentenac, Phenomenological theory of filtering by resonant dielectric gratings, J. Opt. Soc. Amer. A 19 (2002) 1136–1144.
[23] M. Nevière, D. Maystre, G.H. Derrick, R.C. McPhedran, M.C. Hutley, On the total absorption of unpolarized monochromatic light, in: Proceedings of I.C.O. XI Conference, Madrid, Spain, 1978, pp. 609–612.
[24] N. Bonod, G. Tayeb, D. Maystre, S. Enoch, E. Popov, Total absorption of light by lamellar metallic gratings, Opt. Express 16 (2008) 15431–15438.
[25] M.C. Hutley, Diffraction Gratings, Academic Press, 1982.
[26] G.H. Derrick, R.C. McPhedran, D. Maystre, M. Nevière, Crossed gratings: A theory and its applications, Appl. Phys. 18 (1979) 39–52.
[27] E. Hutter, J. Fendler, Exploitation of localized surface plasmon resonance, Adv. Mater. 16 (19) (2004) 1685–1706.
[28] E. Popov, N. Bonod, S. Enoch, Comparison of plasmon surface waves on shallow and deep metallic 1D and 2D gratings, Opt. Express 15 (2007) 4224–4237.
[29] M. Nevière, R. Reinisch, Electromagnetic study of the surface-plasmon-resonance contribution to surface-enhanced Raman scattering, Phys. Rev. B 26 (1982) 5403–5408.
[30] R. Reinisch, M. Nevière, Electromagnetic theory of diffraction in nonlinear optics and surface enhanced nonlinear optical effects, Phys. Rev. 28 (1983) 1870–1885.
[31] E.L. Wood, J.R. Sambles, N.P. Cotter, S.C. Kitson, Diffraction grating characterization using multiple-wavelength excitation of surface-plasmon polaritons, J. Mod. Opt. 42 (1995) 1343–1349.
[32] F. Pincemin, J.-J. Greffet, Propagation and localization of a surface plasmon polariton on a finite grating, J. Opt. Soc. Amer. B 13 (1996) 1499–1509.
[33] W.L. Barnes, S.C. Kitson, T.W. Preist, J.R. Sambles, Photonic surfaces for surface-plasmon polaritons, J. Opt. Soc. Amer. A 14 (1997) 1654–1661.
[34] E.A. Smith, R.M. Corn, Surface plasmon resonance imaging as a tool to monitor biomolecular interactions in an array based format, Appl. Spectr. 57 (2003) 320A–332A.
[35] D.C. Cullen, C.R. Lowe, A direct surface plasmon-polariton immunosensor: preliminary investigation of the non-specific adsorption of serum components to the sensor surface, Sens. Actuators B 1 (1990) 576–579.
[36] D. Maystre, M. Saillard, Localization of light by randomly rough surfaces: Concept of localiton, J. Opt. Soc. Amer. A 11 (1994) 680–690.